Nano Energy (2015) 11, 1–10

Available online at www.sciencedirect.com

ScienceDirect

journal homepage: www.elsevier.com/locate/nanoenergy

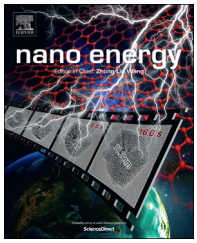

RAPID COMMUNICATION

Highly anisotropic power generation in piezoelectric hemispheres composed stretchable composite film for self-powered motion sensor

Jinsung Chun[a], Na-Ri Kang[a], Ju-Young Kim[a], Myoung-Sub Noh[b], Chong-Yun Kang[b,c], Dukhyun Choi[d], Sang-Woo Kim[e], Zhong Lin Wang[f], Jeong Min Baik[a,*]

[a]School of Materials Science and Engineering, KIST-UNIST-Ulsan Center for Convergent Materials, Ulsan National Institute of Science and Technology (UNIST), Ulsan, Korea
[b]KU-KIST Graduate School of Converging Science and Technology, Korea University, 145, Anam-ro, Seongbuk-gu, Seoul, 136-701, Korea
[c]Electronic Materials Research Center, KIST, Hwarangno 14-gil 5, Seongbuk-gu, Seoul, 137-791, Korea
[d]Department of Mechanical Engineering, College of Engineering, Kyung Hee University, 1 Seocheon-dong, Giheung-gu, Yongin-si, 446-701, Republic of Korea
[e]School of Advanced Materials Science and Engineering, Sungkyunkwan University (SKKU), Suwon 440-746, Republic of Korea
[f]School of Materials Science and Engineering, Georgia Institute of Technology, Atlanta, Georgia 30332-0245, United States

Received 16 July 2014; received in revised form 20 September 2014; accepted 4 October 2014
Available online 27 October 2014

KEYWORDS
Anisotropic;
Hemispheres;
Piezoelectrics;
Stretchable;
Composite;
Nanogenerator

Abstract
Highly-stretchable piezoelectric hemispheres composed composite thin film nanogenerators are fabricated as a self-powered, exceptionally sensitive sensor for providing sensitive motion information from a human body. The composite films are based on the highly-ordered piezoelectric hemispheres embedded in a soft matrix, polydimethylsiloxane (PDMS) and generate large power output up to 6 V and 0.2 μA/cm^2 under normal bending force. The electrical outputs increase by stacking such hemispheres layer-by-layer. The strain sensitivity of the films differs according to the bending direction, and the high sensitivity is achieved by convex bending for hemisphere composite due to the strong electric dipole alignment. The films

*Corresponding author. Tel.: +82 52 2172324; fax: +82 52 2172309.
E-mail address: jbaik@unist.ac.kr (J. Min Baik).

http://dx.doi.org/10.1016/j.nanoen.2014.10.010

are attached on the surface of a wrist and its output voltage/current density provides the information on the wrist motion.

Introduction

Widespread energy harvesting, generating self-sufficient power from the surrounding environment, such as wind [1], solar [2-6], and geothermal [7], have attracted increased attention in the past decade due to the energy crisis and global warming. Among many technologies, energy harvesting technologies based on the piezoelectric effect, named as piezoelectric nanogenerators [8], have been extensively investigated because of an extended life time, no recharging procedures, and scalability. Over the years, many kinds of nanogenerators have been demonstrated to effectively power commercial light-emitting diodes (LEDs) [9], liquid crystal displays (LCDs) [10], and wireless data transmission [11]. For a wide variety of such applications, most nanogenerators have been fabricated based on various piezoelectric nanostructures including nanowires [12-16], nanotubes [17], and porous structures [18], in which most works have been focused on the nanowires on stretchable substrates such as polyethylene terephthalate (PET) [15]. The nanogenerators have been considered as not only promising energy harvesting devices of effectively scavenging energy from the mechanical source, but also sensitive sensors which can detect the minute force [19] or movement such as breathing [20], and a wide range of biological and chemical species [21,22].

In terms of the nanogenerators, a high flexibility or stretchability is essential in generating high-power continuous electric output signals. The high flexibility can provide an opportunity applicable to a target object without any limitation of its shape and movement. Several research efforts have demonstrated the realization of nanogenerators with high flexibility in which the polymer-mold-supporting nanogenerators [15] fabricated using various nanostructured piezoelectric materials such as ZnO [15], $BaTiO_3$ [23], $KNbO_3$ [24], $ZnSnO_3$ [25], and $NaNbO_3$ [26] have been considered as one of promising platforms for the large-scale and super-flexible nanogenerators. However, they are still difficult to be utilized as an efficient approach for super-flexible nanogenerators owing to the high-cost and the low-throughput process. Actually, the most composite-type nanogenerators have been based on the nanowires [26] and nanoparticles [25,26]. For the nanowires, the synthesis methods are available only for a limited number of piezoelectric materials such as ZnO and GaN. Furthermore, it also takes a long time ($\sim$ several hours) to synthesis such nanowires by a hydrothermal method, a well-known process for the growth [23-27]. The power generation of nanoparticles-embedded nanogenerators is critically dependent on the mode of the applied force and it is likely to be mostly feasible only under large pushing force and/or after an electrical poling treatment [23]. Thus, it is necessary to develop innovative strategies applicable to any target objects regardless of the mode and magnitude of the applied force.

Here, we report on extremely stable and directional anisotropic power generation in the composite-type piezoelectric nanogenerators without any treatment of electrical poling. The key innovation of our material design consists of the highly-ordered piezoelectric hemispheres and polydimethylsiloxane (PDMS). Under convex bending motion, the nanogenerator with single hemisphere layer generates an output voltage of up to 4 V and a current density of 0.13 $\mu A/cm^2$, which increases up to 6 V and 0.2 $\mu A/cm^2$ by stacking three layers of such hemispheres layer-by-layer. However, the electrical signal is about 8 times smaller at concave bending. This unique and high directional anisotropic power generation is so desirable for the detection of human body motion, which may offer significant potentials to develop directional sensing approaches for the postural instability and gait disturbance, as well as to generate applicable power from human body motion. The hemisphere structure also enables the composite film to elastically deform and recover upon the application and release of external force, thereby, generating stable output power.

Experimental

Production of piezoelectric hemisphere shapes

An aqueous suspension of 0.5, 1, 3, and 10-μm-diameter polystyrene (PS) beads (2.6 wt%, Polysciences, Warrington, USA) was used to prepare close-packed monolayer beads template for the fabrication of crescent shape periodic structures embedded in the polydimethylsiloxane (PDMS) layer. The SiO_2/Si substrate was treated with UV/Ozone (AHTECH LTS, South Korea) to make the surface of the substrate hydrophilic. Langmuir–Blodgett deposition of the PS beads was done for single layer films, and then the samples were dried for 24 h in a dry box at room temperature. We found that the slow drying process was essential in obtaining monolayer beads template without sphere-free regions or agglomeration. A 100 nm-thick ZnO film was deposited on the PS spheres at room temperature by a RF sputtering. The base pressure, working pressure, rf power, and gas flow rate were 1×10^{-6} Torr, 4 mTorr, 16/4 sccm (Ar/O_2), respectively. A 100 nm-thick piezoelectric lead zirconate titante (PZT) film was also deposited at room temperature by the RF sputtering, in which the deposition power, base pressure, working pressure, and Ar flow rate were maintained at 80 W, 2×10^{-6} Torr, 3 mTorr, and 30 sccm, respectively. The samples were calcined in air at 300 °C for 60 min to burn out the polymer beads and simultaneously crystallize the films, resulting in embossed films

with hollow hemispheres on the substrate. The PZT film was then additionally annealed at 650 °C for 5 min in O_2 ambient (10 Torr) to enhance the crystallization of the materials.

The schematic diagrams of the stretchable composites fabrication process are shown in Fig. 1a and detailed information described in Methods. Scanning electron microscopy (SEM) images in Fig. 1b shows that the 2D ZnO hollow hemisphere arrays are hexagonally close-packed as a form of multi-domains which fill the entire substrate of $>10\,cm^2$ area in the current study. After the piezoelectric-PDMS film is detached from the substrate, piezoelectric hemispheres are clearly shown (Fig. 1c). The PDMS solution was then poured into the hemispheres and allowed to solidify into an amorphous free-standing film by heating on a hot plate at 90 °C. The parameters such as the lift force, speed, and precision are carefully controlled and optimized not to get any space between the hemispheres and the PDMS, as shown in Fig. 1d. This fabrication method for such stretchable composites is broadly applicable to a range of piezoelectric or ferroelectric materials such as lead zirconate titanate (PZT). Actually, we will show the electrical output performance of PZT hemispheres-embedded nanogenerators. The microstructure of the ZnO hemispheres was characterized by low- and high-resolution transmission electron microscopy (TEM), as shown in Figs. 1e, f, and g. The hemisphere clearly reveals

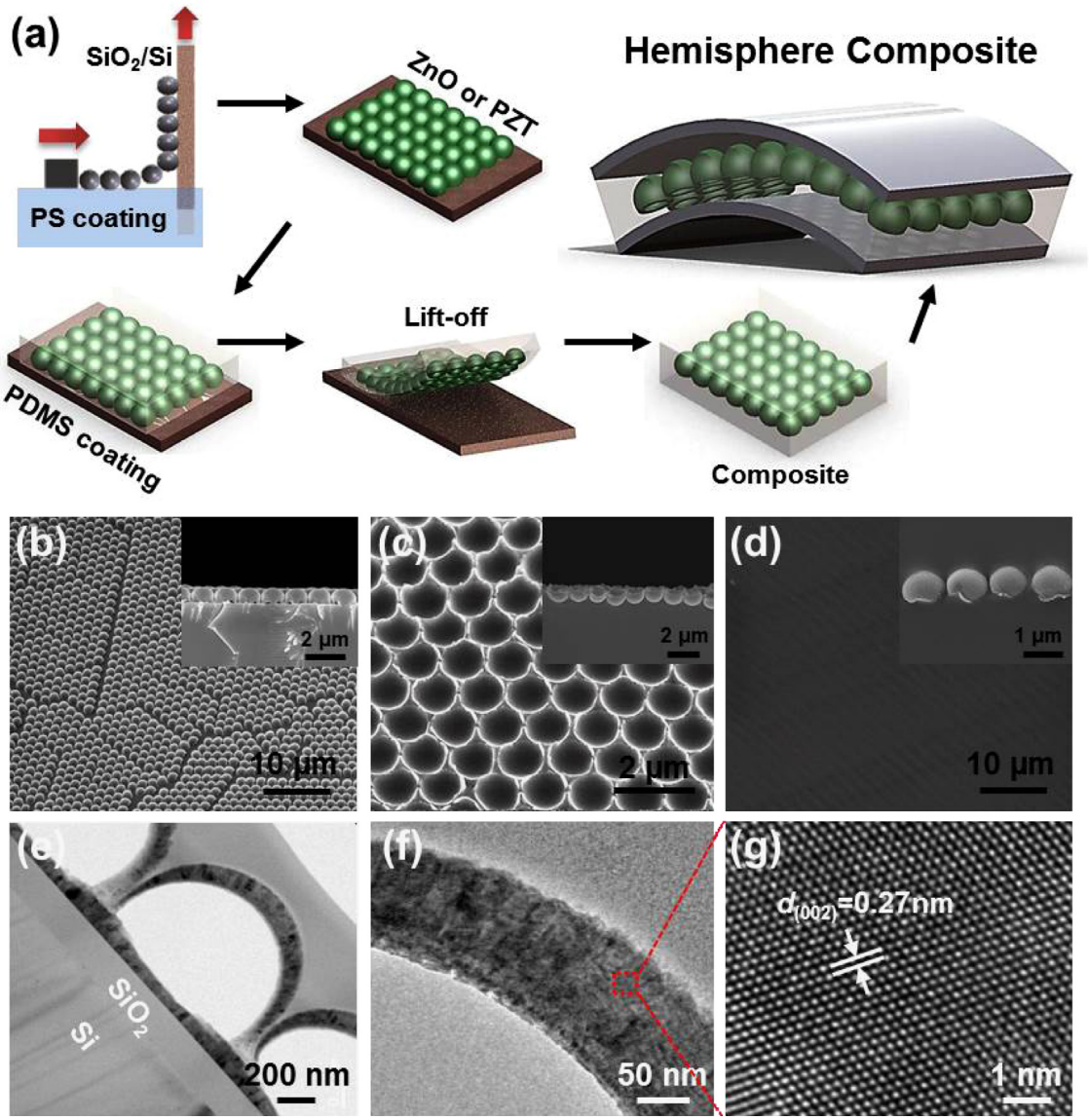

Fig. 1 (a) Schematic diagrams of the fabrication process for the piezoelectric hemispheres embedded stretchable composites. SEM images of (b) hexagonally close-packed 2D ZnO hollow hemisphere arrays as a form of multi-domains of areas larger than approximately $>10\,cm^2$, (c) detached hemisphere array from the substrate, and (d) piezoelectric hemispheres embedded composites. (e) A cross-sectional TEM image results of ZnO hemispheres, which reveal that the hemispheres are hollow. (f) The HR-TEM images also show that the hemisphere has columnar structures with grain sizes in the range of 10–20 nm. (g) High crystallinity of each grain, based on facts that the most part of the grains is bright in dark field image and lattice fringes are well ordered.

fan-shaped columnar structures with grain sizes in the range of 10–20 nm. Each grain shows to be highly crystalline, based on the facts that the most part of the domains is bright in dark field image, lattice fringes are well ordered.

Fabrication of hemisphere embedded composites

The PDMS solution was poured into the PS sphere template and allowed to solidify into an amorphous free-standing film by heating on a hotplate at 90 °C. The PDMS film was then detached from the substrate and soaked in acetone for 24 h to remove the PS spheres, producing free-standing PDMS film with crescent-shape structures. To fabricate composite-type devices, the crescent shape structures were filled by another PDMS layer without any voids between the piezoelectric materials and PDMS. ITO/PET films are then attached on the top and bottom sides of the structures, which act as the top and bottom electrodes. A nanogenerator was also made by stacking two pieces of the structures.

Measurement of electrical performance

We measured the output voltage and current density of the embossed thin film generators under bending condition, which are detected by a Keithley 6485 picoammeter and Keithley 2182A nanovoltmeter of 10 GΩ resistances were used. The effective piezoelectric coefficient (d_{33}) of the hemisphere PZT thin films was measured using a piezoelectric force microscopy (PFM, Dimension 3100, Veeco Instruments, USA) with a lock-in amplifier (SR830, Stanford Research). The piezoelectric responses were collected with a conductive Pt/Ir coated Si tip cantilever (PPP-NCHPt, Nanosensors) with the spring constant 43 N/m and resonance frequency 263 kHz. Piezoelectric response curves were obtained in contact mode, with a typical modulation AC signal frequency with 17 kHz and amplitude with 0.5 V under applied DC bias from −8 V to 8 V.

Microstructural analysis

The morphologies of the composite films with crescent shape structures were characterized by a Nano 230 field emission scanning electron microscope (FEI, USA). Transmission electron microscopy was performed using a transmission electron microscope (JEOL, Japan). A dual-beam focus ion beam (FEI, USA) was used to prepare the TEM samples. High-resolution XRD using synchrotron radiation was carried out to characterize the microstructures of the films at the 3D beamline at Pohang Accelerator Laboratory. Piezoelectric hysteresis properties were measured by a commercial atomic force microscope (XE-100, Park systems, South Korea) with lock-in amplifier (SR830, Stanford Research System) under ambient conditions. For in-situ tension test, a force applied when the crescent-shape composite was stretched was measured by using the tensile tester (AGS-100N, Shimadzu, Japan) under conditions of a speed of 5 mm/min at a distance of 5 mm.

Results and discussion

Figs. 2a and b show the output voltage and current density, generated by the ZnO hemispheres embedded composites as a function of the diameter of the hemispheres from 0.5 to 10 μm under the normal bending direction of 0.425% strain, as shown in the inset of the Fig. 2. The size of active area in nanogenerator is approximately 1.5 × 1.5 cm^2 and the thickness of the composites is fixed to approximately 100 μm. For ZnO film embedded composites, there is no significant change in both voltage and current density although there is a little change ($<$ 0.15 V and $<$0.001 μA/cm^2) by the bending direction. The composite containing the 0.5 μm-diameter ZnO hemispheres in the PDMS matrix generated 0.4 V and 0.13 μA/cm^2 in the output voltage and the current density, respectively, showing almost 4 times improvement in the power generation compared to that of ZnO film-embedded composite. As the diameter of the hemispheres increases, it is clearly seen that the power significantly increases and the composite with 10 μm-diameter hemispheres produces an almost 27 times improvement (4 V and 0.13 μA/cm^2) in the power generation, compared with the ZnO film embedded composite.

The above measurement was repeated with PZT hemispheres (see the Supplementary materials Fig. S1a) embedded composites and we observed similar results, also plotted in Figs. 2a and b. The composite containing 10 μm-diameter PZT hemispheres generated the 3 V and 0.05 μA/cm^2 in the output voltage and the current density, respectively although it showed the output performance lower than that of the ZnO hemispheres embedded composite. Interestingly, the electrical signals are obtained without any treatment of electrical poling. In general, the composite materials, in which piezoelectric materials such as $ZnSnO_3$, $BaTiO_3$, and PZT are embedded, require a high applied force or the treatment of electrical poling to generate high electrical outputs [23,25,27,28]. This may imply that it is more likely to deform elastically under small external force, leading to the stress-induced poling effect [29,30]. The microstructure and piezoelectric characteristics of the PZT hemispheres were also evaluated. In XRD spectra (Fig. S1b), there are two peaks corresponding to the (110) and (200) planes of PZT, but the intensity are not high, meaning that the crystallinity of the materials need to be improved. The piezoelectric response phase and strain amplitude were obtained on the top of the PZT hemispheres. The phase and amplitude signal exhibit typical 180° domain switching behavior under changing polarity of DC bias as shown in the Supplementary materials Fig. S2a. The effective piezoelectric coefficient (d_{33}) is extracted from the phase and amplitude signal (see the Supplementary materials Fig. S2b). The d_{33}-V curve shows clear hysteresis loop because the ferroelectric domain of the PZT thin films are switched under DC bias and the piezoelectric deflection of the films are changed along the polarization alignment with disturbance of remnant polarization. Thus, the optimization process where several factors such as the crystallinity of the materials, the poling process to align the electric dipoles along vertical direction are involved, will increase the electrical output signals generated by the composites.

The detail power generation mechanism of the hemispheres embedded composites is described in Fig. 2c. We calculated the piezopotential distributions inside the composites along the vertical direction by using a simple rectangular model composed of 10 μm-diameter hemispheres with 100 nm-thick ZnO film in a PDMS matrix of

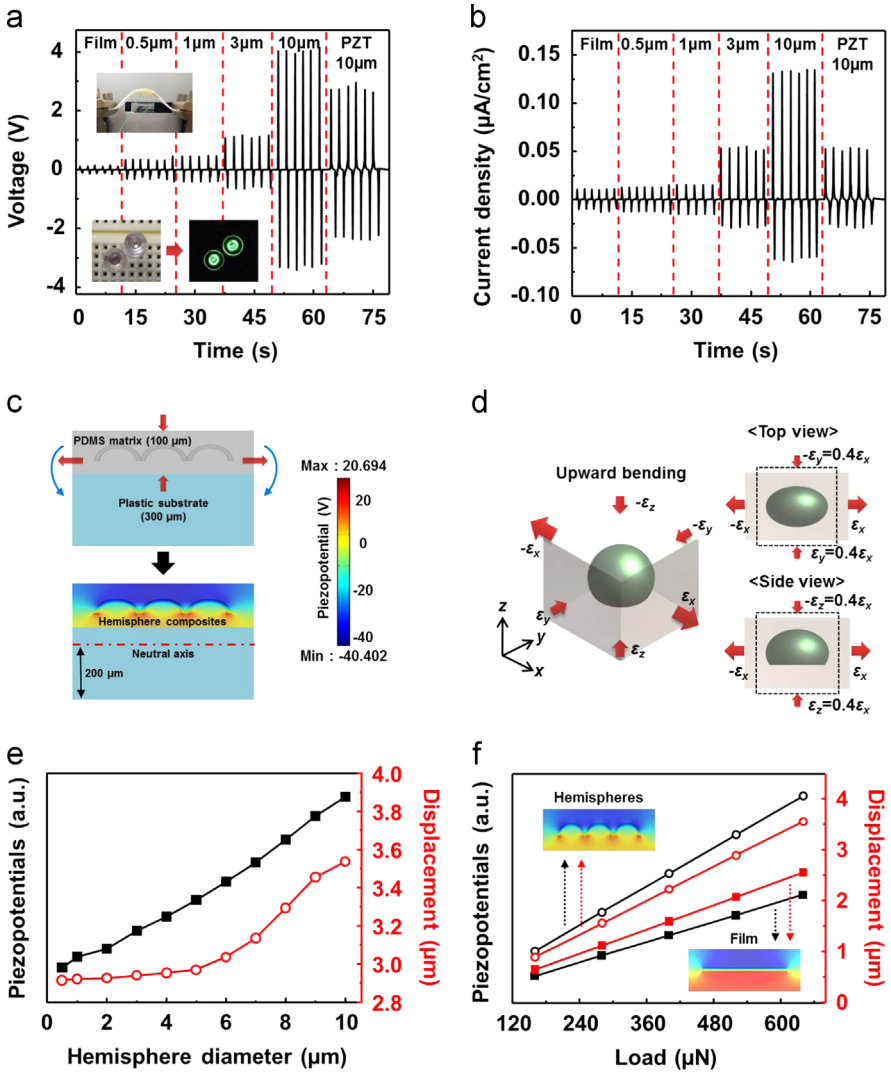

Fig. 2 (a) Output voltage and (b) current density, generated by the ZnO hemispheres embedded composites as a function of the diameter of the hemispheres from 0.5 to 10 μm and PZT hemispheres under the convex bending strain. (c) Piezopotential and (d) strain distributions of hemispheres in PDMS matrix. (e) Piezopotentials and displacement increase with the hemisphere diameter from 0.5 to 10 μm. (f) Enhancement in the piezopotential and displacement as increase of external force from 160 to 640 μN.

100 μm on the substrate of 300 μm under the load of 640 μN. The material parameters of the ZnO and PDMS, taken from the COMSOL simulation software, are used for the finite element analysis. The dielectric constant is 8.5446 and the conductivity is not included because of assuming ZnO materials as insulator. When the composites are under convex bending, Fig. 2c shows the piezopotential distribution in PDMS materials. That is, the tensile stress is built-up over the entire PDMS matrix along the transverse direction, causing the tensile strain to the ZnO hemispheres along the direction. The compressive stress on the hemispheres along the vertical direction is also induced and promotes the strain distribution along the vertical direction, causing a gradient in the piezoelectric potential. If the tensile strain in the transverse direction under convex bending is defined as $\varepsilon = \Delta x/x$, the compressive strain (ε_z) in the vertical direction can be calculated to be $-0.4\varepsilon_x$ by using the Poisson ratio ($\nu = -\varepsilon_{transverse}/\varepsilon_{vertical} = -\varepsilon_y/\varepsilon_x = -\varepsilon_z/\varepsilon_x = 0.4$) of the PDMS material [31], as shown in Fig. 2d. The simulation in Fig. 2e supports that as the hemisphere diameter increases, the displacement of the hemisphere along the vertical direction also increases, resulted in a larger piezoelectric potential. This increase in the displacement may ascribe to the enhancement of the strain confinement effect in larger hemisphere, thereby, strain is likely to be concentrated in larger hemisphere [18]. Furthermore, it was reported that randomly distributed nanoparticles or nanowires in the PDMS matrix might not generate large output power due to the random orientation in the electric dipoles without any treatment of electrical poling and high applied force [32]. Actually, it may be a challenging task to disperse them uniformly inside the matrix. Here, the hemispheres are well-ordered in the PDMS matrix, generating high electrical outputs without any poling treatment. In Fig. 2f, hemisphere composite has the 2 times higher piezopotential and displacement than that of flat film under the load from 160 to 640 μN. Hemisphere composite can generate higher piezopotential,

because hemisphere structure causes more displacement than the flat film structure.

Fig. 3a shows the stability and durability test of 10 μm-diameter ZnO hemispheres embedded composite. It is clearly seen that the output voltage, quite stable, does not appear to change significantly after 500 bending cycles. This result reveals the robustness and mechanical durability of the composite. For further evaluation of the resistance to deformation of the composite by external force, micro-scale uniaxial tensile tests were conducted. Figs. 3b and c show micro-scale uniaxial tensile sample and engineering stress-strain curves for PMDS film, hemisphere composite, and PET film. Dog-bone shaped tensile samples with gage width of 1 mm and gage length of 5 mm were prepared, and uniaxial tensile testing was carried out at a rate of 0.5 mm/min using micro-universal testing machine (AGS-100N, Shimadzu Ltd., Japan). PET film shows significant transition from elastic to elasto-plastic deformation at ~7% engineering strain during tensile loading, as shown in inset of Fig. 3c. On the contrary, the PDMS film and the composite film show linear elastic behavior up to 40% engineering strain that is the maximum strain we tested. By linear fitting to loading curve up to 40% engineering strain, elastic modulus of the PDMS film and the composite film are calculated to be 1.13 MPa and 0.91 MPa, respectively. Although the fracture strain of ZnO hemisphere layer in the composite film is much smaller than that of the PDMS films, the adhesion strength between the ZnO hemispheres and PDMS matrix inside the composite film is quite high. In this case, elastic modulus of composite materials can be calculated by the rule-of-mixture. Elastic modulus of ZnO on the order of 100 GPa is five orders of magnitude greater than that of PDMS on the order of 1 MPa. However, by considering the extremely low volume fraction of the hemisphere layer in composite, the enhancement in elastic modulus is calculated as only 24%. Besides, the composite film stretched up to 40% engineering strain returns back to origin point in stress-strain curve as the pristine PDMS films, indicating the reversible deformation. Thus, the composite film seems to be quite stretchable.

For the high-output performance of the piezoelectric composites, nanogenerators were also made by stacking two and three layers of such hemispheres layer-by-layer. It was also done by Langmuir–Blodgett deposition of the PS on the hemispheres, followed by the deposition of ZnO film. As the number of the hemisphere layers increase, the output voltage and the output current density are enhanced up to 6.0 V and 0.2 $\mu A/cm^2$, respectively, at three-layer stacked nanogenerator, as shown in Figs. 4a and b. This means that this stacking process will make high-output nanogenerator possible. The simulation result in Fig. 4c which shows the increase in the piezopotential as the number of stacking layers increase supports the increase of the electrical outputs with the number of the layers. Also it is worth mentioning that when the overturned hemispheres are stacked on the hemispheres, the output voltage and the output current density decrease up to 1.8 V and 0.04 $\mu A/cm^2$, respectively. These values are much smaller than those obtained in single layered composite film.

To investigate the decrease in the electrical outputs, the same electrical measurement was done with the direction of the bending, convex and concave. Figs. 5a and b show the

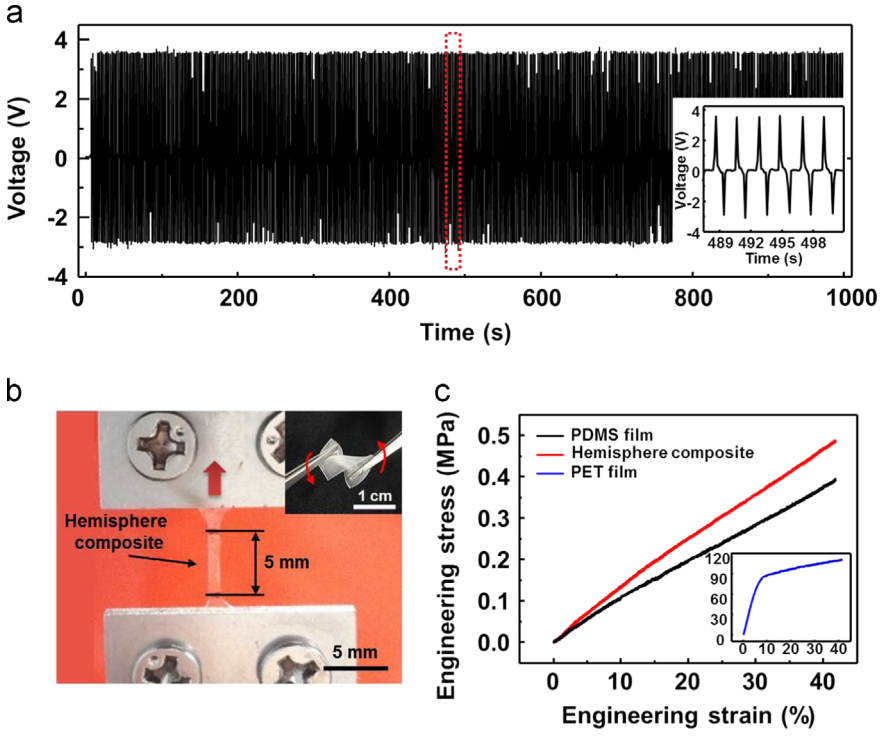

Fig. 3 (a) The stability and durability test of 10 μm-diameter ZnO hemispheres embedded composites. (b) Optical image of micro-scale uniaxial tensile sample and (c) engineering stress-strain curves for PMDS film, hemisphere composite, and PET film.

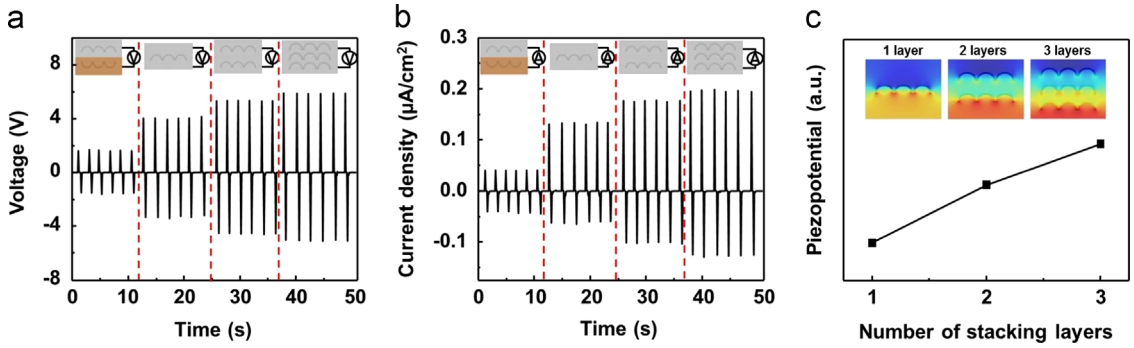

Fig. 4 (a) Output voltage and (b) current density of integrated hemisphere composite by stacking two and three layers of hemispheres layer-by-layer. (c) Enhancement in the piezopotential as the number of stacking layers increase.

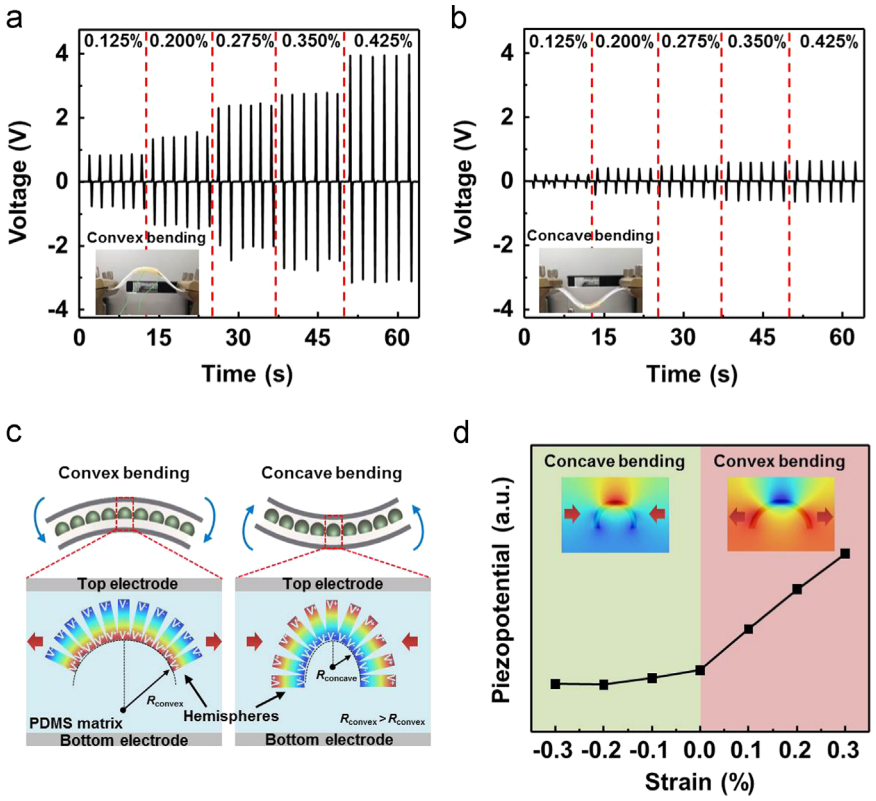

Fig. 5 (a) Output voltages of 10 μm-hemispheres embedded composite film under (a) convex and (b) concave bending with strains from 0.125% to 0.425% with the optical microscope images of the bending direction in the inset. (c) Hemisphere radius (*R*) change and (d) piezopotential distributions under concave and convex bending.

output voltages of 10 μm-hemispheres embedded composite film measured by varying the bending direction under same condition with strains from 0.125 to 0.425%, as shown in the inset of Fig. 5. When the film is under convex bending, the voltage increases from 0.8 V to 4 V with the strains, while when the film is under concave bending, and the voltage is only generated from 0.17 V to 0.52 V. That is, the output voltage is about 8 times higher at convex bending. We found that the data was quite reproducible after doing several same experiments. This result may be understood by considering two factors. The composite is located at the upper part (see the Fig. 2c) of the entire nanogeneator, so that compressive strain is induced along the vertical direction in composite at the convex bending (see the Fig. 2d), as shown in Fig. 5c, and promotes the strain distribution along the direction, resulted in a larger piezoelectric potential at convex bending. According to the neutral axis theory [33], the stress distributions significantly depend on the position of the neutral axis, which is determined from the condition that the resultant axial force acting on the cross section is zero, as shown in Fig. 2c. Therefore, the position of the hemispheres plays an important role in the enhancement of the output power. The more the distance from the neutral axis to the hemispheres increases, the more the corresponding stress in the hemispheres increases.

In the TEM images, the hemisphere reveals fan-shaped columnar structures, meaning that the piezopotential direction is also fan-shaped when it is strained. When the

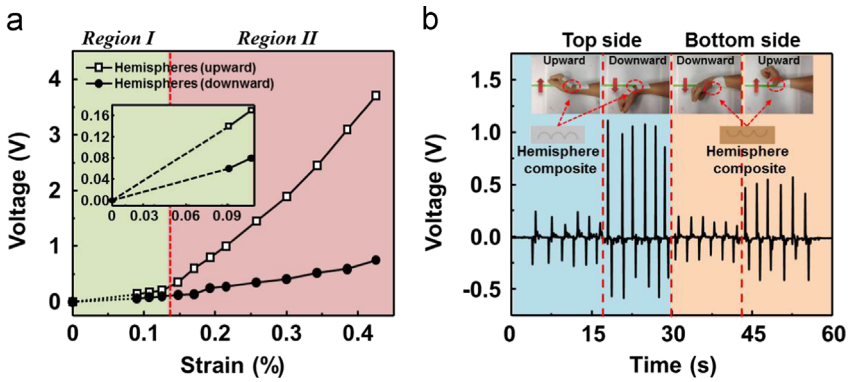

Fig. 6 (a) Bending strain response of the composites for bending direction as the strain increases from 0% to 0.425%. (b) Output voltages of hemisphere composites attached on the top and bottom side of the wrist with a sticking plaster under the bending direction.

composite is under convex bending, the radius of hemisphere (R_{convex}) will increase and the piezopotential each column will be vertically well-aligned. However, at concave bending, the radius of hemisphere decreases ($R_{concave}$) and the piezopotential of each column becomes dispersive, decreasing the net piezopotential to the vertical direction. Fig. 5d shows the piezopotentials of hemisphere composites under convex and concave bending. At convex bending, the piezopotentials is about 2 times higher, consistent with the experimental results. For the simplified numerical calculation, we assumed that ZnO hemisphere is an insulator and is epitaxially grown along the c axis, as shown in Fig. 5d, so that the free charge carriers in the volume can be ignored. A dielectric constant of 10.2 and a piezoelectric coefficient (d_{33}) of 11.7 pC/N are taken from COMSOL software. The simulation shows about 1.5 times higher value under convex bending than that under concave bending. Reduced magnitude of the experimental results in Figs. 2 and 5 in comparison to the simulated value is due to the screening effect of the free carriers within hemisphere [34].

Fig. 6a shows the bending strain response of the composites for two bending directions as the strain increases from 0% to 0.425%. The strain sensitivity S can be defined to be $S=(V_b - V_o)/V_o$, where V_b and V_o denote the output voltage with and without applied force, respectively. Here, in our instrument, V_o is usually measured as approximately 0.01 V. The sensitivity of the composites at the convex bending was substantially larger than those at concave bending. In the $<0.14\%$ strain (Region I), it seems that the output voltages of both cases are not significant, however, at very small strain (even smaller strain than 0.01%), it is obvious that the output voltages of the composites at the convex bending ($S=13$ at 0.09%) are larger than those ($S=5$ at 0.09%) at the concave bending, in which the 0.09% is the lowest value of the instrument, by considering the bending angle limitation. This result shows the ultrasensitive strain sensors providing the information regarding to the bending direction. In the $>0.14\%$ strain (Region II), the output voltage of the composites at the convex bending was substantially 4 times larger than that of the composites at the concave bending. The composites with a size of 15 mm $\times$ 15 mm were firmly attached on the top side of the wrist with a sticking plaster and the output voltages were measured with the bending directions, plotted in Fig. 6b. The composites produced the output voltage of 1.1 V when the wrist is under convex bending, while at the concave bending, the composites produced only 0.25 V. The composites (see the Fig. 6b) were also attached on the bottom side of the wrist and the measurement was repeated, and we observed similar results. These merits provide great potential for an ultrasensitive electronic platform such as self-powered smart skin and the directional bending sensor with an enhanced sensitivity.

Conclusions

In summary, we report highly-stretchable composite-type nanogenerators with the highly-ordered piezoelectric hemispheres in a soft matrix, PDMS. The hemispheres are produced by a Langmuir–Blodgett deposition of 2D PS spheres on planar substrates, followed by the deposition of piezoelectric film by a radio-frequency magnetron sputtering method at room temperature and post-annealing to remove spheres. This fabrication method is broadly applicable to a range of piezoelectric or ferroelectric materials. The composites have a high mechanical durability with good stretchable properties, comparable to the PDMS film. The nanogenerators with single hemisphere layer generated an output voltage of up to 4 V at a current density of 0.13 $\mu A/cm^2$, which increased up to 6 V and 0.2 $\mu A/cm^2$ by stacking three layers of such hemispheres layer-by-layer. The strain sensitivity of the films differs according to the bending direction and high sensitivity is achieved by convex bending due to the strong electric dipole alignment. The films are also attached on the surface of a wrist and its output voltage/current provides information on the wrist direction. The very high sensitivity, small workable strain range, and simple fabrication of the sensors, based on highly-stretchable piezoelectric composite films, make them promising candidates for electronic-skin application, especially, to develop directional sensing approaches for the instability and gait disturbance occurred commonly in patients with Alzheimer's disease, Parkinson's disease, and related disorders.

Acknowledgements

This work was financially supported by the National Research Foundation of Korea (NRF) grant funded by the Ministry of Education, Science and Technology (MEST) (2012R1A2A1A01002787), the KIST-UNIST partnership program (2V03870) or equivalently by the 2014 Research Fund (1.140019.01) of UNIST (Ulsan National Institute of Science and Technology), and the Pioneer Research Center Program through the National Research Foundation of Korea funded

by the Ministry of Science, ICT & Future Planning (NRF-2013M3C1A3063602).

Appendix A. Supporting information

Supplementary data associated with this article can be found in the online version at http://dx.doi.org/10.1016/j.nanoen.2014.10.010.

References

[1] S. Lee, S.H. Bae, L. Lin, Y. Yang, C. Park, S.W. Kim, S.N. Cha, H. Kim, Y.J. Park, Z.L. Wang, Adv. Funct. Mater. 23 (2012) 2445–2449.
[2] S. Jeong, E.C. Garnett, S. Wang, Z. Yu, S. Fan, M.L. Brongersma, M.D. McGehee, Y. Cui, Nano Lett. 12 (2012) 2971–2976.
[3] Y. Yang, H. Zhang, S. Lee, D. Kim, W. Hwang, Z.L. Wang, ACS Nano 7 (2013) 2808–2813.
[4] B. O'Regan, M. Gratzel, Nature 353 (1991) 737–740.
[5] W.U. Huynh, J.J. Dittmer, A.P. Alivisatos, Science 295 (2002) 2425–2427.
[6] Q. Pei, G. Yu, C. Zhang, Y. Yang, A.J. Heeger, Science 296 (1995) 1086–1088.
[7] Y. Yang, W. Guo, K.C. Pradel, G. Zhu, Y. Zhou, Y. Zhang, Y. Hu, L. Lin, Z.L. Wang, Nano Lett. 12 (2012) 2833–2838.
[8] Z.L. Wang, J. Song, Science 312 (2006) 242–246.
[9] G. Zhu, J. Chen, T. Zhang, Q. Jing, Z.L. Wang, Nat. Commun 5 (2014) 3426.
[10] Y. Hu, Y. Zhang, C. Xu, G. Zhu, Z.L. Wang, Nano Lett. 10 (2010) 5025.
[11] T. Chen, L. Qiu, Z. Cai, F. Gong, Z. Yang, Z. Wang, H. Peng, Nano Lett. 11 (2012) 2572.
[12] S. Lee, R. Hinchet, Y. Lee, Y. Yang, Z.H. Lin, G. Ardila, L. Montes, M. Mouis, Z.L. Wang, Adv. Funct. Mater. 24 (2014) 1163–1168.
[13] G. Zhu, A.C. Wang, Y. Liu, Y. Zhou, Z.L. Wang, Nano Lett. 12 (2012) 3086–3090.
[14] S. Lee, S.H. Bae, L. Lin, Y. Yang, C. Park, S.W. Kim, S.N. Cha, H. Kim, Y.J. Park, Z.L. Wang, Adv. Funct. Mater. 23 (2012) 2445–2449.
[15] L. Lin, Y. Hu, C. Xu, Y. Zhang, R. Zhang, X. Wen, Z.L. Wang, Nano Energ. 2 (2013) 75–81.
[16] S. Lee, J.I. Hong, C. Xu, M. Lee, D. Kim, L. Lin, W. Hwang, Z. L. Wang, Adv. Mater. 24 (2012) 4398–4402.
[17] Z.H. Lin, Y. Yang, J.M. Wu, Y. Liu, F. Zhang, Z.L. Wang, J. Phys. Chem. Lett. 3 (2012) 3599–3604.
[18] S. Cha, S.M. Kim, H. Kim, J. Ku, J.I. Sohn, Y.J. Park, B.G. Song, M.H. Jung, E.K. Lee, B.L. Choi, J.J. Park, Z.L. Wang, J.M. Kim, K. Kim, Nano Lett. 11 (2011) 5142–5147.
[19] J. Chun, K.Y. Lee, C.Y. Kang, M.H. Kim, S.W. Kim, J.M. Baik, Adv. Funct. Mater. 24 (2014) 2038–2043.
[20] Z. Li, G. Zhu, R. Yang, A.C. Wang, Z.L. Wang, Adv. Mater. 22 (2010) 2534–2537.
[21] X. Xue, Y. Nie, B. He, L. Xing, Y. Zhang, Z.L. Wang, Nanotechnology 24 (2013) 225501.
[22] R. Yu, C. Pan, J. Chen, G. Zhu, Z.L. Wang, Adv. Funct. Mater. 23 (2013) 5868–5874.
[23] K.I. Park, M. Lee, Y. Liu, S. Moon, G.T. Hwang, G. Zhu, J.E. Kim, S.O. Kim, D.K. Kim, Z.L. Wang, K.J. Lee, Adv. Mater. 24 (2012) 2999–3004.
[24] J.H. Jung, C.Y. Chen, B.K. Yun, N. Lee, Y. Zhou, W. Jo, L.J. Chou, Z.L. Wang, Nanotechnology 23 (2012) 375401.
[25] K.Y. Lee, D. Kim, J.H. Lee, T.Y. Kim, M.K. Gupta, S.W. Kim, Adv. Funct. Mater. 24 (2014) 37–43.
[26] C.K. Jeong, I. Kim, K.I. Park, M.H. Oh, H. Paik, G.T. Hwang, K. No, Y.S. Nam, K.J. Lee, ACS Nano 7 (2013) 11016–11025.
[27] J.H. Jung, M. Lee, J.I. Hong, Y. Ding, C.Y. Chen, L.J. Chou, Z.L. Wang, ACS Nano 5 (2011) 10041–10046.
[28] K.I. Park, C.K. Jeong, J. Ryu, G.T. Hwang, K.J. Lee, Adv. Energ. Mater 3 (2013) 1539–1544.
[29] K. Tetsuo, K. Yukihiro, M. Hideo, K. Makoto, Appl. Phys. Lett. 72 (1998) 608.
[30] A. Gruverman, B.J. Rodriguez, A.I. Kingon, R.J. Nemanich, A.K. Tagantsev, J.S. Cross, M. Tsukada, Appl. Phys. Lett. 83 (2003) 728.
[31] T. Kan, K. Matsumoto, I. Shimoyama, Nanotechnology 23 (2012) 315201.
[32] H. Sun, H. Tian, Y. Yang, D. Xie, Y.C. Zhang, X. Liu, S. Ma, H. Zhao, T.L. Ren, Nanoscale 5 (2013) 6117–6123.
[33] S. Lee, J.Y. Kwon, D. Yoon, H. Cho, J. You, Y.T. Kang, D. Choi, W. Hwang, Nanoscale Res. Lett. 7 (2012) 256.
[34] Y. Gao, Z.L. Wang, Nano Lett. 9 (2009) 1103–1110.

Jinsung Chun is a Ph.D. candidate under the supervision of Prof. Jeong Min Baik at School of Materials Science and Engineering, Ulsan National Institute of Science and Technology (UNIST). His doctoral research focuses on the development of ordered porous structure based piezoelectric generators/triboelectric generators for sustainable energy conversions, self-powered sensor, and fundamental study.

Na-Ri Kang is a Combined Master's-Ph.D candidate under the supervision of Prof. Ju-Young Kim at School of Materials Science and Engineering, Ulsan National Institute of Science and Technology (UNIST). Her doctoral research focuses on improvement of hydrogen sensor using hollow-structured zinc oxide with high volume-to-surface area, and mechanical reliability due to flexibility enhanced by nanostructure and materials size effect.

Dr. Ju-Young Kim is now Assistant Professor in School of Materials Science and Engineering, Ulsan National Institute of Science and Technology (UNIST). He received his Ph.D. from Seoul National University in Department of Materials Science and Engineering in 2007. His recent research interest focuses on the development of multifunctional materials with innovative mechanical, electrical, optical, and chemical performances. His research interests are characterization of mechanical properties of materials at multi-scales and at harsh environments, nanoporous metal-based energy materials for photocatalysis and water splitting systems. And particular interests are reliability issues in flexible electronic devices and MEMS.

Myoung-Sub Noh is a Combined Master's-Ph. D candidate under the supervision of Prof. Chong-Yun Kang at KU-KIST Graduate School of Converging Science and Technology in Korea University. His doctoral research focuses on the development of the flexible piezoelectric thin films energy harvesters and actuators using laser lift-off(LLO) and excimer laser annealing(ELA) methods.

Dr. Chong-Yun Kang received his Ph.D. from the Department of Electrical Engineering of Yonsei University in 2000. Now he is a Principal Research Scientist in KIST from 2000 and a professor of KU-KIST Graduate School of Converging Science and Technology in Korea University from 2012. His research interests include smart materials and devices, especially, piezoelectric energy harvesting and actuators, electrocaloric effect materials, and nanostructured oxide semiconductor gas sensors.

Dr. Dukhyun Choi is now Assistant Professor in Department of Mechanical Engineering, Kyung Hee University. He received his Ph.D. from Pohang University in Department of Mechanical Engineering in 2006. His research interests include the fabrication and a variety of applications of nanostructures and nanomaterials. He focuses on the novel design and the development of hybrid nanocomposite structures for various energy, electronic, and biological devices.

Dr. Sang-Woo Kim is now Associate Professor in School of Advanced Materials Science & Engineering and SKKU Advanced Institute of Nanotechnology (SAINT), and SKKU Young Fellow at Sungkyunkwan University (SKKU). He received his Ph.D. from Kyoto University in Department of Electronic Science and Engineering in 2004. Prof. Kim pioneered the realization of large-scale transparent flexible piezoelectric nanogenerators for harvesting mechanical energy in nature for self-powering of low power-consuming portable and body-implanted electronics. His recent research interest focuses on piezoelectric/triboelectric nanogenerators, piezophototronics, and 2D layered materials including graphene, h-BN, MoS_2, etcetera.

Dr. Zhong Lin Wang received his Ph.D. from Arizona State University in physics. He now is the Hightower Chair in Materials Science and Engineering, Regents' Professor, Engineering Distinguished Professor and Director, Center for Nanostructure Characterization, at Georgia Tech. His research on self-powered nanosystems has inspired the worldwide effort in academia and industry for studying energy for micro-nano-systems, which is now a distinct disciplinary in energy research and future sensor networks. He coined and pioneered the field of piezotronics and piezo-phototronics by introducing piezoelectric potential gated charge transport process in fabricating new electronic and optoelectronic devices.

Dr. Jeong Min Baik is now Associate Professor in School of Materials Science and Engineering, Ulsan National Institute of Science and Technology (UNIST). He received his Ph.D. from Pohang University in Department of Materials Science and Engineering in 2006. His recent research interest focuses on the synthesis of nanomaterials and nanostructures such as nanoparticles, nanowires, nanolayers, and nanopores for the applications of Energy-Conversion Devices and Nano-photonic Devices. Particular interests are concerned with the development of Piezoelectric/Triboelectric Nanogenerators and Artificial Photosynthesis.